Hidden fermion as milli-charged dark matter in Stueckelberg Z' model

Kingman Cheung * and Tzu-Chiang Yuan †

Department of Physics, National Tsing Hua University, Hsinchu, Taiwan

Physics Division, National Center for Theoretical Sciences, Hsinchu, Taiwan

(Dated: January 16, 2007)

Abstract

We augment the hidden Stueckelberg Z' model by a pair of Dirac fermions in the hidden sector, in which the Z' has a coupling strength comparable to weak scale coupling. We show that this hidden fermion-antifermion pair could be a milli-charged dark matter candidate with a viable relic density. Existing terrestrial and astrophysical searches on milli-charged particles do not place severe constraints on this hidden fermion. We calculate the flux of monochromatic photons coming from the Galactic Center due to pair annihilation of these milli-charged particles and show that it is within reach of the next generation γ-ray experiments. The characteristic signature of this theoretical endeavor is that the Stueckelberg Z' boson has a large invisible width decaying into the hidden fermion-antifermion pair. We show that existing Drell-Yan data do not constrain this model yet. Various channels of singly production of this Z' boson at the LHC and ILC are explored.

* Email address: cheung@phys.nthu.edu.tw
† Email address: tcyuan@phys.nthu.edu.tw

I. INTRODUCTION

The standard model (SM) of particle physics has been blessed with her elegant way of giving masses to the weak gauge bosons by the Higgs mechanism. However, the crucial ingredient of this mechanism, the Higgs boson, is still missing. In addition, a scalar Higgs boson mass is not stable under perturbative calculation. It will receive an enormous amount of radiative corrections to its mass such that a delicate cancellation between its bare mass and radiative corrections is needed so as to obtain a mass in the electroweak scale – this is the famous hierarchy problem. An alternative way to give mass to an abelian $U(1)$ gauge boson is known as the Stueckelberg mechanism. Although it is very difficult to give masses to nonabelian gauge bosons without sacrificing renormalizability within the Stueckelberg approach, it is worthwhile to study the consequence of this mechanism as an extension to the SM with extra abelian $U(1)$ factors.

Recently, Kors and Nath [1] showed that the SM extended by a hidden sector described by a Stueckelberg $U(1)_X$ and the gauge field C_μ associated with it can pass all the existing constraints from electroweak data as well as direct search limits from the Tevatron. Through the combined Stueckelberg and Higgs mechanisms, the SM $SU_L(2) \times U(1)_Y$ gauge fields B_μ and W^3_μ mix with the hidden sector gauge field C_μ. After rotation from the interaction basis (C_μ, B_μ, W^3_μ) to the mass eigenbasis (Z'_μ, Z_μ, A_μ), one obtains a massless state identified to be the photon γ and two massive eigenstates which are the SM-like Z boson and an additional Z' boson. As long as the mixing is small, the Z' boson only couples very weakly to the SM fermions, and so it can evade all the existing constraints on conventional Z' models. The allowed mass range for the Stueckelberg Z' can be anywhere from 200 GeV to a few TeV [2]. Typically, the mass of the Stueckelberg Z' is above the SM Z boson mass.

In this work, a pair of hidden Dirac fermions is introduced in the Stueckelberg Z' model. Such a possibility has been mentioned in Ref.[1], but its phenomenology was not explored. There could be various types or generations of fermions in the hidden sector, just like our visible world. Since the abelian $U(1)_X$ is assumed to be the only gauge group in the hidden sector and there is no connector sector between our visible world and the hidden one in this class of models, all hidden fermions in this sector are stable. [1] Thus the hidden fermion-

[1] This is in analogous to the pure QED case, muon does not decay into an electron plus a photon.

antifermion pair that we add in the model can be viewed as the lightest ones in the hidden sector, should there be more than one type of them. The SM fermions are neutral under this hidden $U(1)_X$. Since this hidden fermion pair is stable, it can be the dark matter candidate of our Universe.

In the next Section, we will present some details of the Stueckelberg Z' extension of the SM with an additional pair of Dirac fermion-antifermion in the hidden sector. In Section III, we discuss milli-charged dark matter. Treating the hidden fermion as our candidate of dark matter, we calculate its relic density and explore the parameter space allowed by the WMAP measurement. We also calculate the monochromatic photon flux coming from the Galactic Center due to pair annihilation of these hidden fermions. In Section IV, we explore some novel collider phenomenology of the Stueckelberg Z' with the presence of the hidden fermion. Since the width of the Stueckelberg Z' is no longer narrow, compared to the scenario studied in [2], its phenomenology is rather different. Comments and conclusions are given in Section V.

II. THE MODEL

The Stueckelberg extension [1] of the SM (StSM) is obtained by adding a hidden sector associated with an extra $U(1)_X$ interaction, under which the SM particles are neutral. [2] We explicitly specify the content of the hidden sector: a gauge boson C_μ and a pair of fermion and antifermion χ and $\bar{\chi}$.

The Lagrangian describing the system is $\mathcal{L}_{\rm StSM} = \mathcal{L}_{\rm SM} + \mathcal{L}_{\rm St}$, where

$$\begin{aligned}
\mathcal{L}_{\rm SM} &= -\frac{1}{4} W^a_{\mu\nu} W^{a\mu\nu} - \frac{1}{4} B_{\mu\nu} B^{\mu\nu} - D_\mu \Phi^\dagger D^\mu \Phi - V(\Phi^\dagger \Phi) \\
&\quad + i\bar{\psi}_f \gamma^\mu D_\mu \psi_f \ , \qquad (1) \\
\mathcal{L}_{\rm St} &= -\frac{1}{4} C_{\mu\nu} C^{\mu\nu} + i\bar{\chi}\gamma^\mu D^X_\mu \chi - \frac{1}{2} \left(\partial_\mu \sigma + M_1 C_\mu + M_2 B_\mu\right)^2 \ , \qquad (2) \\
D_\mu &= \partial_\mu + i g_2 \frac{\tau^a}{2} W^a_\mu + i g_Y \frac{Y}{2} B_\mu \ , \qquad (3) \\
D^X_\mu &= \partial_\mu + i g_X Q_X C_\mu \ , \qquad (4)
\end{aligned}$$

where $W^a_{\mu\nu} (a = 1, 2, 3)$, $B_{\mu\nu}$, and $C_{\mu\nu}$ are the field strength tensors of the gauge fields W^a_μ,

[2] It was shown in Ref. [1] that the SM fermions are neutral under the extra $U(1)_X$ has the advantage of maintaining the neutron charge to be zero.

B_μ, and C_μ, respectively. The SM fermions f were explicitly forbidden from carrying the $U(1)_X$ charges, as implied by Eq. (3), while the hidden fermion pair only carries the $U(1)_X$ charge, as implied by Eq. (4). One can show that the scalar field σ decouples from the theory after gauge fixing terms are added upon quantization.

The mass term for $V \equiv (C_\mu,\, B_\mu,\, W_\mu^3)^T$, after electroweak symmetry breaking $\langle\Phi\rangle = v/\sqrt{2}$, is given by [1]

$$-\frac{1}{2}V^T M V \equiv -\frac{1}{2}\left(C_\mu,\, B_\mu,\, W_\mu^3\right)\begin{pmatrix} M_1^2 & M_1 M_2 & 0 \\ M_1 M_2 & M_2^2+\frac{1}{4}g_Y^2 v^2 & -\frac{1}{4}g_2 g_Y v^2 \\ 0 & -\frac{1}{4}g_2 g_Y v^2 & \frac{1}{4}g_2^2 v^2 \end{pmatrix}\begin{pmatrix} C_\mu \\ B_\mu \\ W_\mu^3 \end{pmatrix} . \tag{5}$$

A similarity transformation can bring the mass matrix M into a diagonal form

$$\begin{pmatrix} C_\mu \\ B_\mu \\ W_\mu^3 \end{pmatrix} = O\begin{pmatrix} Z'_\mu \\ Z_\mu \\ A_\mu \end{pmatrix} \quad , \qquad O^T M\, O \,= \mathrm{diag}(m_{Z'}^2,\, m_Z^2,\, 0)\,. \tag{6}$$

The $m_{Z'}^2$ and m_Z^2 are given by

$$\begin{aligned} m_{Z',\,Z}^2 \;=\; & \frac{1}{2}\Big[M_1^2 + M_2^2 + \frac{1}{4}(g_Y^2+g_2^2)v^2 \\ & \pm\sqrt{(M_1^2+M_2^2+\frac{1}{4}g_Y^2 v^2+\frac{1}{4}g_2^2 v^2)^2 - (M_1^2(g_Y^2+g_2^2)v^2 + g_2^2 M_2^2 v^2)}\Big]\,. \end{aligned} \tag{7}$$

The orthogonal matrix O is parameterized as [3]

$$O = \begin{pmatrix} c_\psi c_\phi - s_\theta s_\phi s_\psi & s_\psi c_\phi + s_\theta s_\phi c_\psi & -c_\theta s_\phi \\ c_\psi s_\phi + s_\theta c_\phi s_\psi & s_\psi s_\phi - s_\theta c_\phi c_\psi & c_\theta c_\phi \\ -c_\theta s_\psi & c_\theta c_\psi & s_\theta \end{pmatrix}\,, \tag{8}$$

where $s_\phi = \sin\phi, c_\phi = \cos\phi$ and similarly for the angles ψ and θ. The angles are related to the original parameters in the Lagrangian $\mathcal{L}_{\mathrm{StSM}}$ by

$$\delta \equiv \tan\phi = \frac{M_2}{M_1}, \quad \tan\theta = \frac{g_Y\cos\phi}{g_2}, \quad \tan\psi = \frac{\tan\theta\,\tan\phi\, m_W^2}{\cos\theta[m_{Z'}^2 - m_W^2(1+\tan^2\theta)]}\,, \tag{9}$$

where $m_W = g_2 v/2$. The Stueckelberg Z' decouples from the SM when $\phi \to 0$, since

$$\tan\phi = \frac{M_2}{M_1} \to 0 \quad \Rightarrow \quad \tan\psi \to 0 \quad \text{and} \quad \tan\theta \to \tan\theta_{\mathrm{w}}$$

[3] We note that the middle column is chosen to be different from that of Ref.[1] by an overall minus sign.

where $\theta_{\rm w}$ is the Weinberg angle.

The interactions of fermions with the neutral gauge bosons before rotating to the mass eigenbasis are given by

$$-\mathcal{L}_{\rm int}^{NC} = g_2 W_\mu^3 \,\bar{\psi}_f \gamma^\mu \frac{\tau^3}{2}\psi_f + g_Y B_\mu \,\bar{\psi}_f \gamma^\mu \frac{Y}{2}\psi_f + g_X C_\mu \,\bar{\chi}\gamma^\mu Q_X \chi \,, \tag{10}$$

where f denotes the SM fermions. The neutral gauge fields are rotated into the mass eigenbasis using Eq. (8), and the above neutral current interaction becomes

$$\begin{aligned} -\mathcal{L}_{\rm int}^{NC} \;=\; & \bar{\psi}_f \,\gamma^\mu \left[\left(\epsilon_{Z'}^{f_L} P_L + \epsilon_{Z'}^{f_R} P_R\right) Z'_\mu + \left(\epsilon_Z^{f_L} P_L + \epsilon_Z^{f_R} P_R\right) Z_\mu + e Q_{\rm em} A_\mu\right] \psi_f \\ & +\; \bar{\chi}\gamma^\mu \left[\epsilon_\gamma^\chi A_\mu + \epsilon_Z^\chi Z_\mu + \epsilon_{Z'}^\chi Z'_\mu\right] \chi \,, \end{aligned} \tag{11}$$

where

$$\begin{aligned} \epsilon_\gamma^\chi &= g_X Q_X^\chi (-c_\theta s_\phi) \,, \\ \epsilon_Z^\chi &= g_X Q_X^\chi (s_\psi c_\phi + s_\theta s_\phi c_\psi) \,, \\ \epsilon_{Z'}^\chi &= g_X Q_X^\chi (c_\psi c_\phi - s_\theta s_\phi s_\psi) \,, \\ \epsilon_Z^{f_{L,R}} &= \frac{c_\psi}{\sqrt{g_2^2 + g_Y^2 c_\phi^2}} \left(-c_\phi^2 g_Y^2 \frac{Y}{2} + g_2^2 \frac{\tau}{2}\right) + s_\psi s_\phi g_Y \frac{Y}{2} \,, \\ \epsilon_{Z'}^{f_{L,R}} &= \frac{s_\psi}{\sqrt{g_2^2 + g_Y^2 c_\phi^2}} \left(c_\phi^2 g_Y^2 \frac{Y}{2} - g_2^2 \frac{\tau}{2}\right) + c_\psi s_\phi g_Y \frac{Y}{2} \,. \end{aligned} \tag{12}$$

In the above, we have used the relations

$$e = g_2 \, s_\theta = g_Y c_\phi c_\theta \qquad \text{and} \qquad Q_{\rm em} = \frac{\tau^3}{2} + \frac{Y}{2} \,,$$

where $Q_{\rm em}$ is the electric charge operator. From Eqs.(11)–(12), it is clear that in this class of model, the SM fermions interact with the hidden world through Z' and the hidden fermion interacts with our visible world through γ and Z. In our computation, we assume the following input parameters at the electroweak scale [3]

$$\alpha_{\rm em}(m_Z) = \frac{1}{128.91}, \;\; G_F = 1.16637 \times 10^{-5}\,{\rm GeV}^{-2}, \;\; m_Z = 91.1876\,{\rm GeV}\,, \sin^2\theta_{\rm w} = 0.231 \,,$$

and the following three inputs related to the hidden sector

$$\delta \equiv \tan\phi, \;\; g_X, \;\; \text{and} \;\; M_{Z'} \,.$$

Since Q_X^χ always enters in the product form $g_X Q_X^\chi$, one can set Q_X^χ to be unity without loss of generality. We derive from $\alpha_{\rm em}$, G_F, m_Z, and $\sin^2\theta_{\rm w}$ the values of

$$e = \sqrt{4\pi\alpha_{\rm em}} \,, \; v = \left(\sqrt{2} G_F\right)^{-1/2} \,, \; m_W = m_Z \sqrt{1 - \sin^2\theta_{\rm w}} \,, \;\; \text{and} \;\; g_2 = 2 m_W / v \,.$$

We then fix the value of g_Y by the following equation

$$e = \frac{g_2 g_Y c_\phi}{\sqrt{g_2^2 + g_Y^2 c_\phi^2}} \, .$$

The other two angles θ and ψ are determined from the last two formulas in Eq.(9).

It is clear from Eqs. (11)-(12) that the chiral couplings of the SM Z boson are affected by the mixing. In fact, even the mass of the Z boson is modified in this model, as shown by Eq. (7). It has been shown in Ref. [2] that in order to keep the Z boson mass within the experimental uncertainty, the mixing angle must satisfies

$$\delta \lesssim 0.061 \sqrt{1 - (m_Z/M_1)^2} \, . \tag{13}$$

When δ is small and $m_{Z'}$ is large, $M_1 \approx m_{Z'} + O(g_2 v)$. The constraint coming from the electroweak precision data is more or less the same as in Eq. (13) [2].

The limits obtained in Ref. [2] also included the analysis from direct Z' production at the Tevatron. They showed that with the current Drell-Yan data,

$$\begin{aligned} m_{Z'} &> 250 \text{ GeV} \quad \text{for} \quad \delta \approx 0.035 \, , \\ m_{Z'} &> 375 \text{ GeV} \quad \text{for} \quad \delta \approx 0.06 \, . \end{aligned} \tag{14}$$

If including the presence of a hidden fermion that the Stueckelberg Z' can couple to, the limit from direct Z' direction would be relaxed because of the smaller production rate into visible lepton pairs [2]. In Sec. IV, we will show that with a hidden fermion χ that can fulfill the dark matter constraint, the Z' would dominantly decay into the hidden sector fermion pair if the $m_{Z'} > 2m_\chi$. It would therefore entirely remove the constraint in Eq. (14) from direct production. On the other hand, if $m_{Z'} < 2m_\chi$ the Z' boson cannot decay into the hidden sector fermions, and so the constraint in Eq. (14) stands.

In the following numerical works, we will apply the constraints on δ and $m_{Z'}$ given by Eqs. (13) and (14) respectively, but when $m_{Z'} > 2m_\chi$ the latter constraint will be dropped.

III. DARK MATTER PHENOMENOLOGY

A. Milli-charged dark matter

Milli-charged dark matter was first discussed by Goldberg and Hall [4], motivated by the work of Holdom [5] in which milli-charged particles in the hidden sector can interact

with the visible photon due to kinetic mixing between the visible photon and the hidden or shadow photon. Numerous constraints for the milli-charged particles, including accelerator experiments, invisible decay in ortho-positronium, SLAC milli-charged particle search, Lamb shift, big-bang nucleosynthesis, dark matter search, search of fractional charged particles in cosmic rays, and other astrophysical reactions, were summarized in [6] (see Fig. 1 of the first reference in [6]). Study of the constraints on milli-charged charged particles from neutron stars and CMB measurements were discussed in Refs.[7] and [8] respectively. In summary, milli-charged particles of mass from MeV to TeV with a fractional electric charge $(10^{-6} - 10^{-1})$ of a unit charge are still allowed. We note that integral charged dark matter was also contemplated in [9]. More recently, PVLAS [10] reported a positive signal of vacuum magnetic dichroism. It has been suggested [11] that photon-initiated pair production of milli-charged fermions with a mass range between 0.1 to a few eV and a milli-charge $O(10^{-6})$ of a unit charge can explain the signal. However, this signal has not been reproduced by other experiment like [12].

B. Relic density and WMAP measurement

The first set of processes we consider in our relic density calculation are

$$\chi\bar{\chi} \to Z', Z, \gamma \to f\bar{f}$$

where f is any SM fermion. The amplitude for the annihilation $\chi(p_1)\ \bar{\chi}(p_2) \to f(q_1)\ \bar{f}(q_2)$ can be written as

$$\mathcal{M} = \bar{v}(p_2)\,\gamma_\mu\,u(p_1) \times \bar{u}(q_1)\,\gamma^\mu\ (\xi_L P_L + \xi_R P_R)\ v(q_2) \tag{15}$$

where $P_{L,R} = (1 \mp \gamma_5)/2$, and

$$\xi_{L,R} \ = \ \frac{\epsilon_\gamma^\chi e Q_{\rm em}^f}{s} + \frac{\epsilon_Z^\chi \epsilon_Z^{f_{L,R}}}{s - m_Z^2} + \frac{\epsilon_{Z'}^\chi \epsilon_{Z'}^{f_{L,R}}}{s - m_{Z'}^2}\ . \tag{16}$$

The differential cross section is given by

$$\frac{d\sigma}{dz} \ = \ \frac{N_f}{32\pi}\,\frac{\beta_f}{s\beta_\chi}\,\left[(\xi_L^2 + \xi_R^2)(u_m^2 + t_m^2 + 2m_\chi^2(s - 2m_f^2)) + 4\,m_f^2\,\xi_L\xi_R(s + 2m_\chi^2)\right] \tag{17}$$

where $\beta_{f,\chi} = (1 - 4m_{f,\chi}^2/s)^{1/2}$, $N_f = 3\,(1)$ for f being a quark (lepton), $t_m = t - m_\chi^2 - m_f^2 = -s(1-\beta_f\beta_\chi z)/2$, $u_m = u - m_\chi^2 - m_f^2 = -s(1+\beta_f\beta_\chi z)/2$, s is the square of the center-of-mass energy, and $z \equiv \cos\Theta$ with Θ the scattering angle.

We also consider pair annihilation of $\chi\bar{\chi}$ into two neutral gauge bosons,

$$\chi\bar{\chi} \to V_1 V_2 \quad \text{with} \quad V_{1,2} = \gamma,\ Z,\ Z' \tag{18}$$

in our relic density calculation. The differential cross section is given by

$$\begin{aligned}
\frac{d\sigma(\chi\bar{\chi} \to V_1 V_2)}{d\Omega} \;=\; & \frac{S(\epsilon^{\chi}_{V_1})^2(\epsilon^{\chi}_{V_2})^2\beta_{V_1V_2}}{64\pi^2 s\beta_\chi}\Big\{ -2\left(2\,m_\chi^2 + m_{V_1}^2\right)\left(2\,m_\chi^2 + m_{V_2}^2\right)\left(\frac{1}{u_\chi^2} + \frac{1}{t_\chi^2}\right) \\
& +\; 2\left(\frac{t_\chi}{u_\chi} + \frac{u_\chi}{t_\chi}\right) - 4\left(\frac{1}{u_\chi} + \frac{1}{t_\chi}\right)\left(2\,m_\chi^2 + m_{V_1}^2 + m_{V_2}^2\right) \\
& -\; \frac{4}{u_\chi t_\chi}\left(2\,m_\chi^2 + m_{V_1}^2 + m_{V_2}^2\right)\left(2\,m_\chi^2 - m_{V_1}^2 - m_{V_2}^2\right)\Big\}\theta(2m_\chi - m_{V_1} - m_{V_2})
\end{aligned} \tag{19}$$

where $\beta_{V_1V_2} = \lambda^{1/2}\left(1, m_{V_1}^2/s,\, m_{V_2}^2/s\right)$ with $\lambda(a,b,c) = a^2 + b^2 + c^2 - 2(ab + bc + ca)$ the Mandelstam function, t_χ and u_χ are given by $t_\chi = t - m_\chi^2$ and $u_\chi = u - m_\chi^2$ respectively, and S is the statistical factor. We note that processes $\chi\bar{\chi} \to \gamma\gamma, ZZ$ are doubly suppressed by the small mixing angles and $\chi\bar{\chi} \to Z'Z'$ are either suppressed or forbidden by phase space, and therefore their contributions are negligible in the annihilation rates.

The quantity that is relevant in the relic density calculation is the thermal averaged cross section $\langle\sigma v\rangle$, where v is the relative velocity of two annihilating particles. In the non-relativistic approximation $v \simeq 2\,\beta_\chi$. To estimate the relic density of a weakly-interacting massive particle, we use the following formula [13]

$$\Omega_\chi h^2 \simeq \frac{0.1\ \text{pb}}{\langle\sigma v\rangle}\ .$$

With the most recent WMAP [14] result on dark matter density

$$\Omega_{\text{CDM}} h^2 = 0.105 \pm 0.009\ ,$$

where we have used the WMAP-data-only fit and taken $\Omega_{\text{CDM}} = \Omega_{\text{matter}} - \Omega_{\text{baryon}}$, one can translate this WMAP data into

$$\langle\sigma v\rangle \simeq 0.95 \pm 0.08\ \text{pb}\ . \tag{20}$$

In estimating the annihilation rate during the freeze-out, we assume that the species has a velocity-squared $v^2 \simeq 0.1$. To get a crude estimation, we ignore the thermal average and evaluate σv directly.

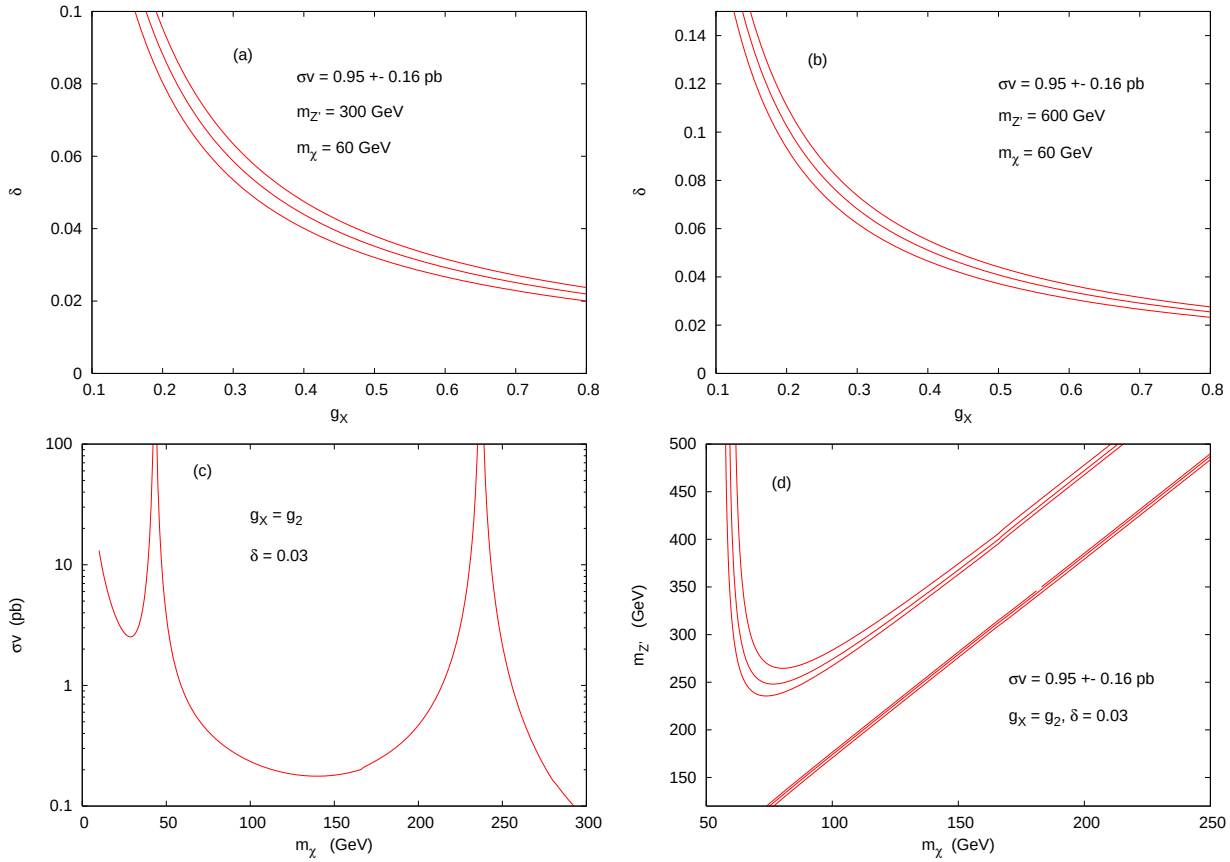

FIG. 1: (a)–(b) are contours of $\sigma v = 0.95 \pm 0.16$ pb (2 σ range) in the plane of (g_X, δ) for various $m_{Z'}$ and m_χ. Part (c) shows the annihilation rate σv versus m_χ with $m_{Z'} = 500$ GeV, $g_X = g_2$, and $\delta = 0.03$. Part (d) shows the contour of $\sigma v = 0.95 \pm 0.16$ pb (2 σ range) in the $(m_\chi, m_{Z'})$ plane.

In Fig.1(a) and (b), we show the contours of $\sigma v = 0.95 \pm 0.16$ pb (2 σ range) in the plane of (g_X, δ) for various input values of $m_{Z'}$ and m_χ. We have included $\chi\bar{\chi} \to \gamma Z', ZZ'$, and $f\bar{f}$, with $f = \nu_e$, ν_μ, ν_τ, e^-, μ^-, τ^-, u, d, s, c, b, and t that are kinematically allowed. We can see, e.g. from part (a) for $m_\chi = 60$ GeV and $m_{Z'} = 300$ GeV, that $\delta = 0.03$ and $g_X \simeq 0.6$ can give the correct amount of dark matter. Similarly, from part (b) a slightly larger $g_X \simeq 0.7$ can do the job. For comparison, we note that $e \simeq 0.31$ and $g_2 \simeq 0.65$ in the SM. Thus, the value of the hidden $U_X(1)$ coupling g_X that we deduced from the WMAP measurement has the same order of the weak coupling g_2. In Fig.1(c), we show the annihilation rate σv versus m_χ for $\delta = 0.03$, $g_X = g_2$, and a fixed $m_{Z'} = 500$ GeV. Clear resonance structures of Z and Z' are seen. In Fig.1(d), we show the contours of σv in the

$(m_\chi, m_{Z'})$ plane. There are two branches: (i) the upper branch where $m_\chi < m_{Z'}/2$ and the band relating m_χ and $m_{Z'}$ is relatively wide; (ii) the lower branch where $2m_\chi > m_{Z'}$ and the band relating m_χ and $m_{Z'}$ is quite narrow. A narrow band implies the need of a fine-tuned relation between m_χ and $m_{Z'}$ in order to give the correct dark matter density. In the latter branch, the Tevatron bound of $m_{Z'} > 250$ GeV for $\delta \approx 0.03$ has to be imposed. Therefore, the case of $m_\chi < m_{Z'}/2$ is more preferred theoretically.

The hidden fermion χ couples to the photon via the mixing angles $c_\theta s_\phi$, the value of which is about $0.9 \times 0.03 \approx 0.03$. Therefore, effectively the fermion χ "acquires" an electric charge of $g_X Q_X^\chi c_\theta s_\phi / e \approx 0.06$, when its coupling to the photon is considered. Therefore, the range of $m_\chi \sim O(100)$ GeV and the size of effective electric charge $\simeq 0.06$ implied by dark matter density requirement in our calculation are consistent with the constraints on milli-charged particles [6].

C. Indirect detection

If milli-charged hidden fermions like χ and $\bar{\chi}$ are the dark matter, their pair annihilation into $\gamma\gamma, \gamma Z$, and $\gamma Z'$ in regions of high dark matter density, e.g. the Galactic Center, can give rise to γ-rays that can reach our Earth for its indirect detection. The cross sections for these processes can be obtained from Eq.(19). The observed γ-ray flux along the line-of-sight between the Earth and the Galactic Center is given by [13]

$$\Phi_\gamma(\psi, E) = \sigma v \frac{dN_\gamma}{dE} \frac{1}{4\pi m_\chi^2} \int_{\text{line of sight}} ds \rho^2(r(s,\psi)) \,, \tag{21}$$

where the coordinate s runs along the line of sight in a direction making an angle ψ from the direction of the Galactic Center, dN_γ/dE is the energy spectrum of the γ-rays, and $v \approx 2\beta_\chi$ is the relative velocity of the dark matter χ and $\bar{\chi}$. The flux from a solid angle $\Delta\Omega$ is often expressed as

$$\Phi_\gamma(\Delta\Omega, E) \approx 5.6 \times 10^{-12} \frac{dN_\gamma}{dE} \left(\frac{\sigma v}{\text{pb}}\right) \left(\frac{1\,\text{TeV}}{m_\chi}\right)^2 \overline{J}(\Delta\Omega) \Delta\Omega \,\text{cm}^{-2}\,\text{s}^{-1} \,, \tag{22}$$

with the quantity $J(\psi)$ defined by

$$J(\psi) = \frac{1}{8.5\,\text{kpc}} \left(\frac{1}{0.3\,\text{GeV/cm}^3}\right)^2 \int_{\text{line of sight}} ds \rho^2(r(s,\psi)) \,. \tag{23}$$

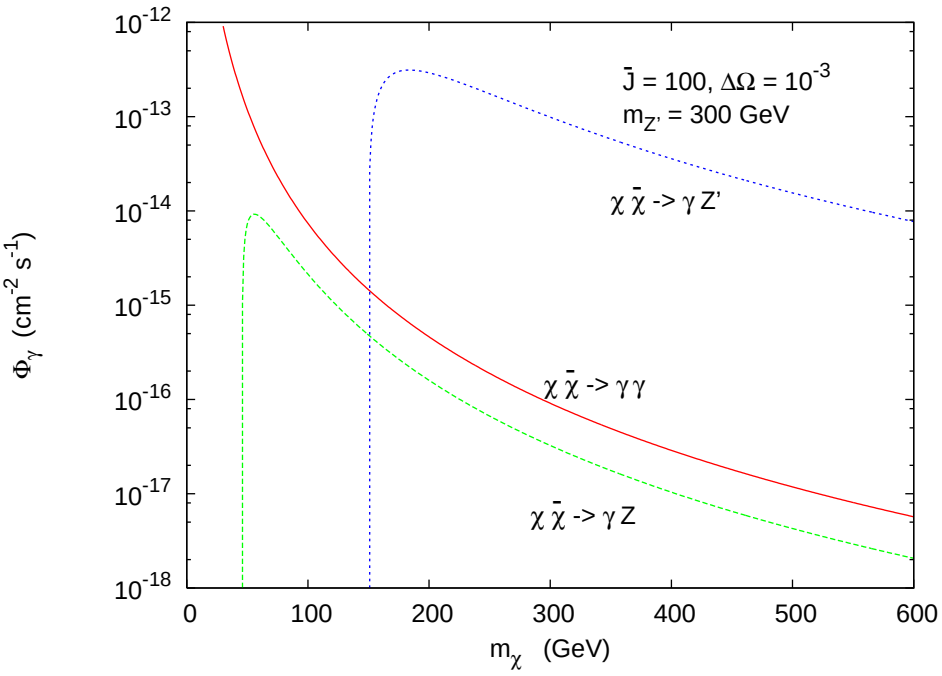

FIG. 2: The resulting flux from annihilation processes $\chi\bar{\chi} \to \gamma\gamma$, γZ, and $\gamma Z'$. We have used typical values of $\overline{J} = 100$ and $\Delta\Omega = 10^{-3}$.

For the process of $\chi\bar{\chi} \to \gamma\gamma$, we would have a mono-energetic γ-ray line with $dN_\gamma/dE \approx 2\delta(E - m_\chi)$. Such a line, if observed, would be a distinctive signal for dark matter annihilation. Similarly, processes $\chi\bar{\chi} \to \gamma Z$ and $\chi\bar{\chi} \to \gamma Z'$ will have a photon energy spectrum as $dN_\gamma/dE \approx \delta(E - m_\chi(1 - m_{Z,Z'}^2/4m_\chi^2))$. The contributions from these processes to the photon flux are shown in Fig. 2, using typical values of $\overline{J} = 100$ and $\Delta\Omega = 10^{-3}$. Unfortunately, the flux of the γ-rays from the process $\chi\bar{\chi} \to \gamma\gamma$ is quite small due to double suppression of $(\epsilon_\gamma^\chi)^2$. The process $\chi\bar{\chi} \to \gamma Z$ contributes at a somewhat lower flux level. The process $\chi\bar{\chi} \to \gamma Z'$ can also contribute to the monochromatic photon flux, provided that $2m_\chi > m_{Z'}$. However, this process is only suppressed by one power of the mixing angle. Potentially, it could be more substantial than the doubly-suppressed process $\chi\bar{\chi} \to \gamma\gamma$. Note that since $2m_\chi > m_{Z'}$ the Tevatron bound Eq.(14) of $m_{Z'} > 250$ GeV for $\delta \approx 0.035$ must be enforced. When kinematics allowed, the photon flux from this process is three orders of magnitude higher than that from $\chi\bar{\chi} \to \gamma\gamma$.

The expected sensitivities for the new Atmospheric Cerenkov Telescope (ACT) experiments such as HESS and VERITAS are at the level of $(10^{-14} - 10^{-13})$ cm^{-2} s^{-1} with an angular coverage of about 10^{-3} [15]. From Fig. 2 there is a small range of m_χ ($m_\chi < 100$

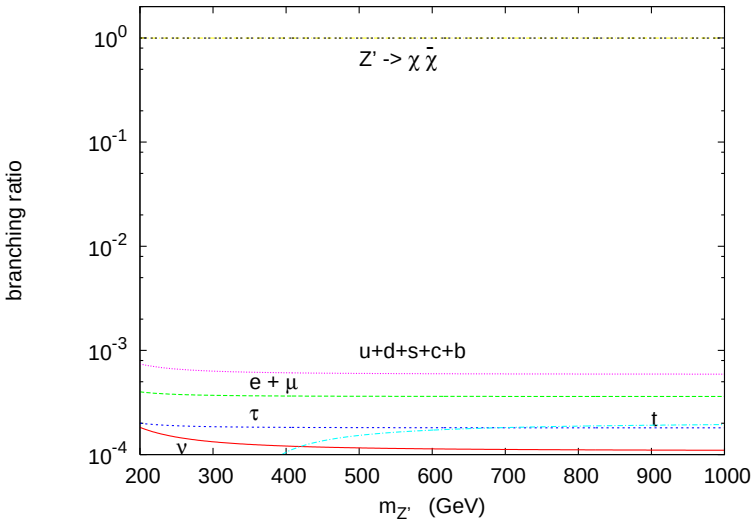

FIG. 3: Branching ratios for Z' with $g_X = g_2$, $\delta = 0.03$, and $m_\chi = 60$ GeV.

GeV) such that $\chi\bar{\chi} \to \gamma\gamma$ contributes at a level larger than 10^{-14} cm^{-2} s^{-1}. The process $\chi\bar{\chi} \to \gamma Z$ contributes at a level below the sensitivity for all range of m_χ, whereas the process $\chi\bar{\chi} \to \gamma Z'$ can contribute at a much larger flux and it is indeed above the sensitivity level for $m_\chi < 600$ GeV.

IV. COLLIDER PHENOMENOLOGY

Phenomenology of the Stueckelberg Z' with the presence of the hidden fermion-antifermion χ and $\bar{\chi}$ that the Z' can decay into is quite different from the one studied before in Refs. [1, 2].

The partial width of Z' into a SM fermion pair $f\bar{f}$ is given by

$$\Gamma(Z' \to f\bar{f}) = \frac{N_f \beta_f}{24\pi} m_{Z'} \left[\left({\epsilon_{Z'}^{f_L}}^2 + {\epsilon_{Z'}^{f_R}}^2 \right) \left(1 - \frac{m_f^2}{m_{Z'}^2} \right) + 6\, \epsilon_{Z'}^{f_L}\, \epsilon_{Z'}^{f_R} \frac{m_f^2}{m_{Z'}^2} \right] \tag{24}$$

and into hidden fermion pair $\chi\bar{\chi}$ is simply

$$\Gamma(Z' \to \chi\bar{\chi}) = \frac{\beta_\chi}{12\pi} m_{Z'} {\epsilon_{Z'}^{\chi}}^2 \left(1 + \frac{2\, m_\chi^2}{m_{Z'}^2} \right) . \tag{25}$$

Here, $\beta_{f,\chi} = (1 - 4m_{f,\chi}^2/m_{Z'}^2)^{1/2}$. The total width of Z' is evaluated by summing over all partial widths, including both the SM modes and the hidden mode. We show in Fig. 3 the various branching ratios for Z' as a function of its mass with the following inputs $g_X = g_2$, $\delta = 0.03$, and $m_\chi = 60$ GeV. Since the mixing angle is so small ($\delta = 0.03$), the Z' is

mainly composed of the C_μ boson of the hidden sector. Hence, the Z' dominantly decays into the hidden sector fermion pair while it has only a small fraction of 10^{-3} into visible fermions. The strategy for the search of this Z' would be very different from all the previous conventional Z' models including the hidden Stueckelberg Z' studied in [1, 2].

Before we explore for the possible collider phenomenology of the Stueckelberg Z' boson and the hidden sector fermion χ, we have to make sure that the new particles and the hidden sector interactions will not upset the existing data.

A. Constraints from invisible decays of Z and quarkonia

Firstly, the SM Z boson that is observed at LEP would decay into a pair of hidden fermions $\chi\bar{\chi}$, giving rise to additional invisible width other than the neutrinos. Because of the mixings among the three neutral gauge bosons, the Z boson can couple to the $\chi\bar{\chi}$ pair via the mixing angle s_ϕ. We have calculated the partial width of $Z \to \chi\bar{\chi}$ for $g_X = g_2$, $\delta = 0.03$ (consistent with the dark matter requirement), and $m_\chi = 0 - 45$ GeV. The partial width is about 0.24 MeV, which is much smaller than the uncertainty 1.5 MeV of the invisible width of the Z boson [3]. Even if we allow a larger mixing angle $\delta = 0.061$ (its maximum value allowed by Eq. (13)), the invisible width of Z would be at most 1 MeV, which is still within the 1σ uncertainty of the data. If the mass of χ is beyond half of the Z boson mass, the invisible width of the Z boson would not constrain the model.

The hidden fermion χ can also couple to the photon via the mixing angles $c_\theta s_\phi$, the maximum of which is about $0.9 \times 0.03 \approx 0.03$. Therefore, effectively the fermion χ "acquires" an electric charge of $g_X Q^\chi_{X\chi} c_\theta s_\phi / e \approx 0.06$ when its coupling to the photon is considered. If χ is very light, of the order of MeV, it could be produced in J/ψ and Υ decays as invisible particles. Constraints on invisible decays of J/ψ and Υ exist (for a comprehensive review on constraints on light dark matter: see Ref. [16]). A very recent update on the $\Upsilon(1S)$ invisible width is given in Ref. [17]. The invisible widths of J/ψ and Υ are respectively

$$B(J/\psi \to \text{invisible}) < 7 \times 10^{-3} \quad \text{and} \quad B(\Upsilon(1S) \to \text{invisible}) < 2.5 \times 10^{-3} \, .$$

However, the partial width of J/ψ into $\chi\bar{\chi}$ is suppressed by the milli-charged factor of $(0.06)^2$ relative to the partial width into e^-e^+. Thus $B(J/\psi \to \chi\bar{\chi}) \approx (0.06)^2 \times B(J/\psi \to e^-e^+) \approx 10^{-4}$, which is well below the above limit. The situation for Υ invisible decay is very similar:

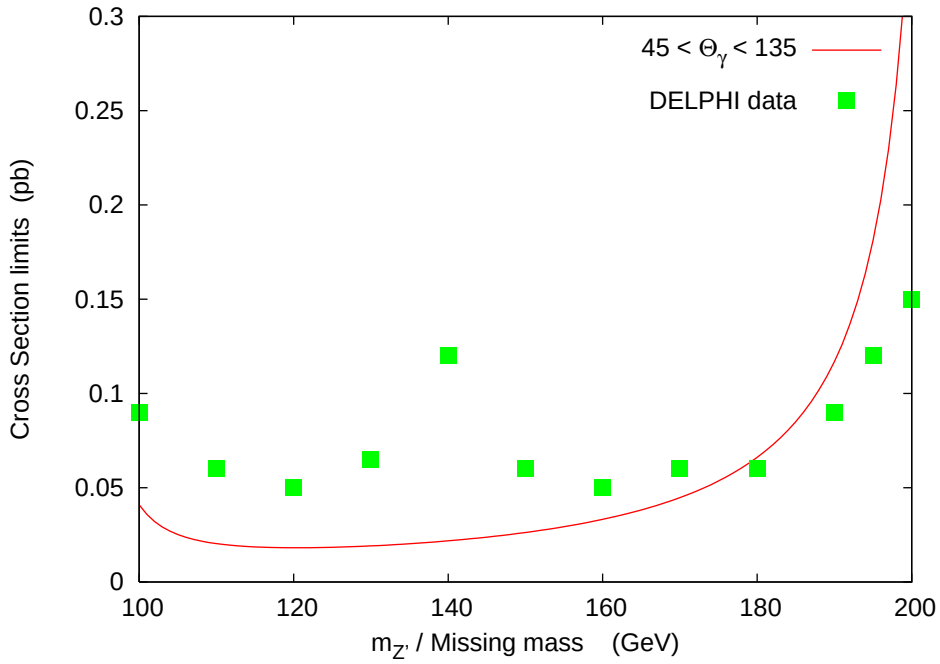

FIG. 4: Comparison with the DELPHI data on the mono-photon production. The theory prediction is for $g_X = g_2$ and $\delta = 0.03$.

$B(\Upsilon(1S) \to \chi\bar{\chi}) \approx (0.06)^2 \times B(\Upsilon(1S) \to e^-e^+) \approx 10^{-4}$, which is also safe. There are also other decays modes, such as J/ψ or $\Upsilon \to \gamma +$ invisible, but it is straightforward to check that with an effective charge of 0.06 the experimental limits of these radiative invisible modes do not constrain the model at all. If the mass m_χ is above 5 GeV, it has no constraint at all from these invisible decays of the quarkonia.

B. Constraint from singly production of Z' at LEPII

Singly production of the Z' at LEPII is possible via $e^-e^+ \to \gamma Z'$ followed by the invisible decay of the Z'. This process is very similar to the SM process $e^-e^+ \to \gamma Z \to \gamma\nu\bar{\nu}$. The differential cross section for $e^-e^+ \to \gamma Z'$ is given by

$$\frac{d\sigma(e^-e^+ \to \gamma Z')}{d\cos\Theta} = \frac{\beta_{Z'} e^2 Q_e^2}{32\pi s}\left(\epsilon_{Z'}^{e_L\,2} + \epsilon_{Z'}^{e_R\,2}\right)\frac{1}{ut}\left[t^2 + u^2 + 2sm_{Z'}^2\right], \tag{26}$$

where Θ is the scattering angle of the photon, $t = -s\beta_{Z'}(1-\cos\Theta)/2$, $u = -s\beta_{Z'}(1+\cos\Theta)/2$, and $\beta_{Z'} = (1 - m_{Z'}^2/s)$. We show the production cross section at LEPII energy $\sqrt{s} = 205$ GeV in Fig. 4 as a function of $m_{Z'}$. Since the Z' would decay into invisible $\chi\bar{\chi}$, the signal of which would be a mono-photon. The recoil mass spectrum would then indicate

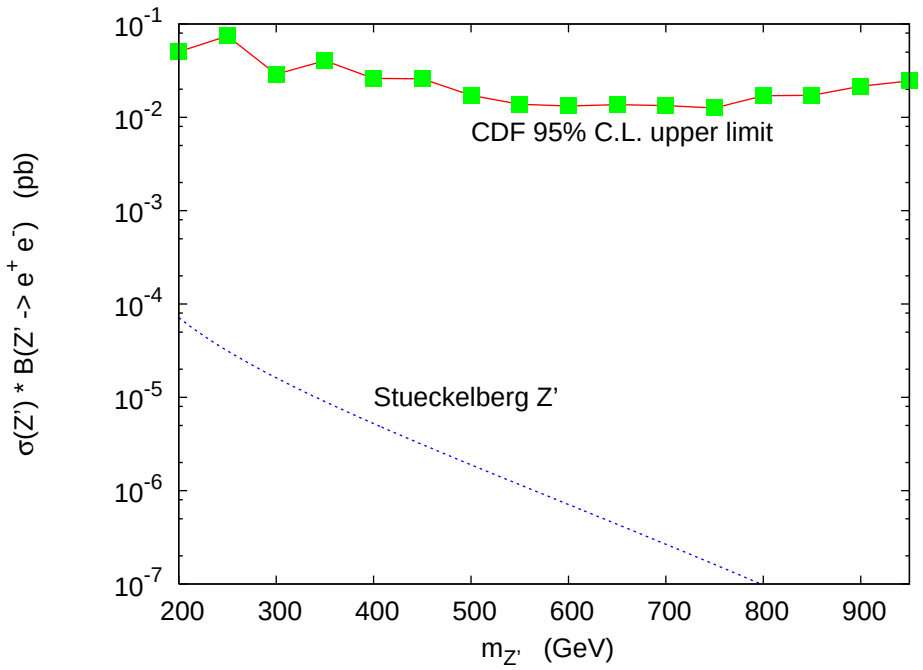

FIG. 5: Drell-Yan cross sections $p\bar{p} \to Z' \to e^- e^+$ versus $m_{Z'}$ for $g_X = g_2$ and $\delta = 0.03$. We also show the 95% C.L. upper limits on $\sigma(Z') \cdot B(Z' \to e^- e^+)$ from the CDF preliminary results [19].

the mass of the Z'. In the figure, we also show the 95% C.L. upper limits on mono-photon production as a function of the missing mass obtained by DELPHI [18]. A small mass range of Z', 180 GeV $\lesssim m_{Z'} \lesssim$ 200 GeV, is disfavored by the data. However, one has to be cautious in this relatively soft photon region where large theoretical uncertainties are expected to be important.

C. Drell-Yan production of Z' at the Tevatron

The production cross section of Z' followed by the leptonic decay at the Tevatron is given by

$$\sigma(p\bar{p} \to Z' \to \ell^- \ell^+) = \frac{1}{144} \frac{1}{s} \frac{m_{Z'}}{\Gamma_{Z'}} \left({\epsilon^{\ell_L}_{Z'}}^2 + {\epsilon^{\ell_R}_{Z'}}^2 \right) \sum_{q=u,d,s,c} \left({\epsilon^{q_L}_{Z'}}^2 + {\epsilon^{q_R}_{Z'}}^2 \right) \int_r^1 \frac{dx}{x} f_q(x)\, f_{\bar{q}}\left(\frac{r}{x}\right) \tag{27}$$

where $\sqrt{s} = 1960$ GeV, $r = m_{Z'}^2/s$, $\Gamma_{Z'}$ is the total width of Z' given in Eqs. (24) and (25), and $\epsilon_{Z'}^{f_{L,R}}$ can be found in Eq. (12). This Drell-Yan cross section for the Z' boson is plotted in Fig. 5, where the 95% C.L. upper limits on $\sigma(Z') \cdot B(Z' \to e^- e^+)$ from the CDF preliminary results [19] are also shown. It is clear that the present CDF limits do

not constrain the model at all. This is in sharp contrast to the results studied in Ref. [2] because the Z' boson that we consider here has a very small branching fraction into charged lepton pair. The Z' boson would decay preferably into the hidden sector fermions instead of visible particles. On the other hand, the Stueckelberg Z' in Ref. [2] only decays into the SM particles. In our case the Z' only has a branching ratio of $\sim 10^{-4} - 10^{-3}$ into leptonic pairs, and it would not be easily detected in the Drell-Yan channel. Neither the hadronic decay modes of Z' can afford it to be detected. Even in the future runs of the Tevatron with a sensitivity reaching the level of $10^{-3} - 10^{-2}$ pb, it is still not possible to detect this kind of Z' boson through the Drell-Yan channel.

D. Singly production of Z' at LHC and ILC

Perhaps one has to rely on the invisible decay mode of the Stueckelberg Z' of this model to identify its presence. Here we calculate the predictions of singly Z' production at the LHC and ILC. Other than the Drell-Yan process that we have considered, the next relevant process to probe this invisible Z' is via $q\bar{q} \to gZ'$ followed by $Z' \to \chi\bar{\chi}$, which gives rise to monojet events. The subprocess cross section can be easily adapted from Eq. (26):

$$\frac{d\hat{\sigma}(q\bar{q} \to gZ')}{d\cos\theta^*} = \frac{\beta_{Z'} g_s^2}{72\pi\hat{s}} \left(\epsilon_{Z'}^{q_L\,2} + \epsilon_{Z'}^{q_R\,2}\right) \frac{1}{\hat{u}\,\hat{t}} \left[\hat{t}^2 + \hat{u}^2 + 2\,\hat{s}\,m_{Z'}^2\right] . \tag{28}$$

Other cross channels, e.g., $qg \to qZ'$, can be obtained from Eq. (28) using the crossing symmetry. The branching ratio $B(Z' \to \chi\bar{\chi})$ is very close to unity. We show in Fig. 6 the production rate of monojet events versus $m_{Z'}$ with $g_X = g_2$ and $\delta = 0.03$ at the LHC under the jet cuts of $p_{Tj} > 20$ GeV and $|\eta_j| < 2.5$. The $q\bar{q}Z'$ coupling is suppressed by the small mixing angle, the same as in the Drell-Yan process, but unlike the Drell-Yan process, this monojet amplitude is suppressed by only one power of the mixing angle instead of two. Therefore, the rate is not negligible. Also, the true SM background for monojet is rather rare. Thus, the monojet event actually signals the presence of such an invisible Z'.

Another place to detect such an invisible Z' is at the ILC with the process $e^-e^+ \to \gamma Z' \to \gamma\chi\bar{\chi}$, which we have considered above for the mono-photon limits from LEP. We extend the energy to $0.5 - 1.5$ TeV and calculate the event rates for the mono-photon final state. We show in Fig. 7 the production rates at $\sqrt{s} = 0.5, 1, 1.5$ TeV with $g_X = g_2$ and $\delta = 0.03$.

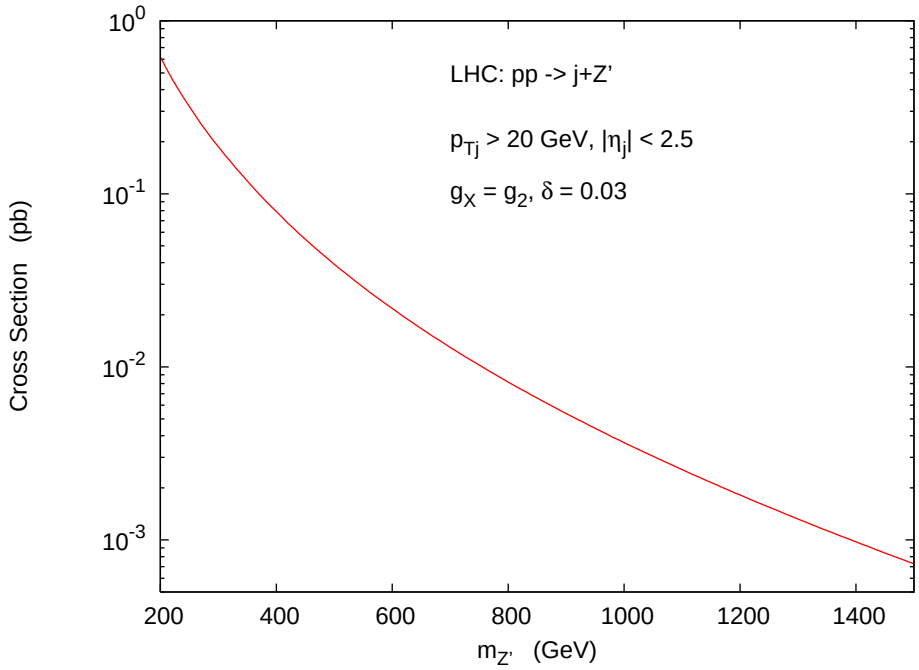

FIG. 6: Production cross section for the process $pp \to j + Z'$ followed by invisible decay of the Z' with $g_X = g_2$ and $\delta = 0.03$ at the LHC. We imposed $p_{Tj} > 20$ GeV and $|\eta_j| < 2.5$ on the jet.

V. CONCLUSIONS

We have proposed an extension of the Stueckelberg Z' standard model by adding a pair of fermion and antifermion in the hidden sector, which has only a $U(1)_X$ symmetry. The stability of the hidden fermion pair with its weak sized interaction makes it a suitable dark matter candidate with a correct amount of dark matter density. We have calculated the photon flux from the Galactic Center due to the annihilation of this milli-charged dark matter. If $2m_\chi < m_{Z'}$, there is only a small range of m_χ that the photon flux is above the sensitivity level of the future γ-ray experiments. However, if $2m_\chi > m_{Z'}$ there is a wide range of m_χ that the photon flux is above the sensitivity level. The collider phenomenology may be different from those studied in Ref. [2], because the dominant decay of the Z' is into the invisible $\chi\bar{\chi}$ if kinematically allowed. In this case, the present Drell-Yan data cannot constrain the model at all. We have proposed the monojet signal at the LHC and the mono-photon signal at the future ILC to probe this invisibly decaying Stueckelberg Z' boson.

A few comments are in order here.

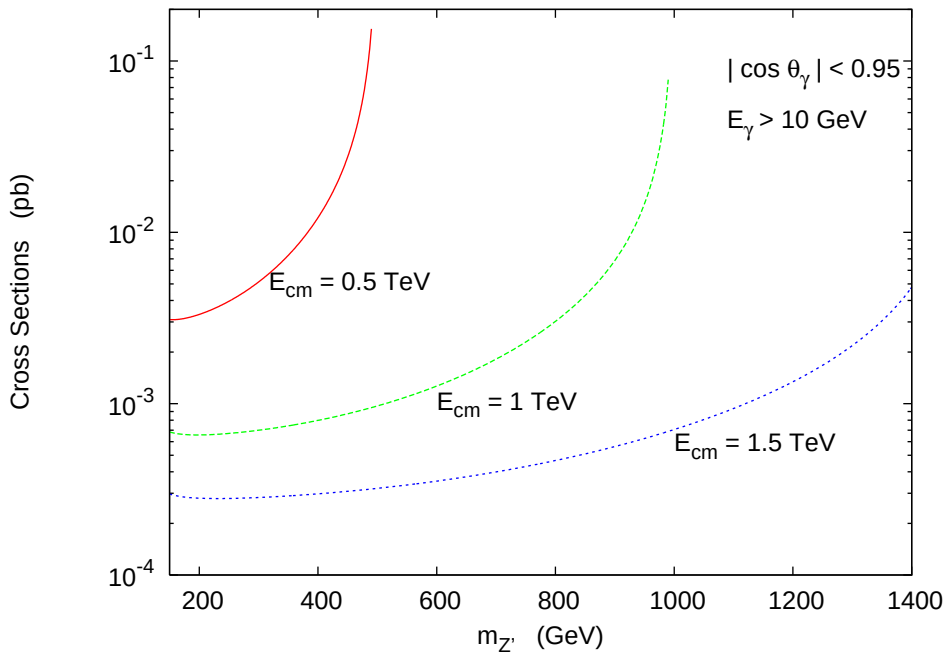

FIG. 7: Production cross section for the process $e^-e^+ \to \gamma + Z'$ followed by invisible decay of the Z' with $g_X = g_2$ and $\delta = 0.03$ at ILC ($\sqrt{s} = 0.5$, 1, 1.5 TeV). We imposed $E_\gamma > 10$ GeV and $|\cos_\gamma| < 0.95$ on the photon.

1. Since only a $U_X(1)$ symmetry is assumed in the hidden sector, each hidden fermion is stable against decay. Therefore, if we assume more hidden fermion pairs in the hidden sector, their relic densities are additive. Thus, a larger coupling constant is needed to ensure larger annihilation cross sections.

2. When $m_{Z'} < 2m_\chi$, the Z' decays dominantly into visible particles. It can be easily detected in the Drell-Yan channel. The existing data constrains the model, as given by Eq. (14) originally obtained by the authors in Ref.[2]. Photon flux from pair annihilation of $\chi\bar{\chi} \to \gamma Z'$ at the Galactic Center is also within reach at the next generation of γ-ray experiments.

3. When $m_{Z'} > 2m_\chi$, the Z' decays dominantly into invisible $\chi\bar{\chi}$. The present Drell-Yan data cannot constrain the model, neither can the invisible decays of J/ψ and Υ for a very light χ. However, the mono-photon production limits obtained by DELPHI disfavors a small range of 180 GeV $\lesssim m_{Z'} \lesssim$ 200 GeV. We anticipate that in the future ILC the missing mass spectrum can efficiently constrain this type of invisibly

decaying Z' boson.

4. The hidden fermion appears to have a milli-charge as it acquires a small effective coupling to the photon through the mixing induced by the combined Higgs and Stueckelberg mechanisms. With a mass of $O(100)$ GeV and an effective charge 0.06 of a unit charge, the hidden fermions are consistent with the existing constraints on milli-charged particles [6]. As milli-charged particle is of very recent interests [11], an update on the terrestrial and astrophysical constraints on this hidden milli-charged particle is desirable.

Acknowledgment

This research was supported in part by the National Science Council of Taiwan R. O. C. under Grant No. NSC 95-2112-M-007-001 and by the National Center for Theoretical Sciences.

---

[1] B. Kors and P. Nath, JHEP **0507**, 069 (2005) [arXiv:hep-ph/0503208]; B. Kors and P. Nath, Phys. Lett. B **586**, 366 (2004) [arXiv:hep-ph/0402047].

[2] D. Feldman, Z. Liu, and P. Nath, Phys. Rev. Lett. **97**, 021801 (2006) [arXiv:hep-ph/0603039].

[3] W.-M. Yao *et al.*, J. Phys. G **33**, 1 (2006).

[4] H. Goldberg and L. J. Hall, Phys. Lett. B **174**, 151 (1986).

[5] B. Holdom, Phys. Lett. B **166**, 196 (1986); Phys. Lett. B **178**, 65 (1986).

[6] S. Davidson, S. Hannestad, and G. Raffelt, JHEP **0005**, 003 (2000) [arXiv:hep-ph/0001179]; S. Davidson, B. Campbell, and D. C. Bailey, Phys. Rev. D **43**, 2314 (1991).

[7] A. Gould, B. T. Draine, R. W. Romani, and S. Nussinov, Phys. Lett. B **238**, 337 (1990).

[8] S. L. Dubovsky, D. S. Gorbunov, and G. I. Rubtsov, JETP Lett. **79**, 1 (2004) [Pisma Zh. Eksp. Teor. Fiz. **79**, 3 (2004)] [arXiv:hep-ph/0311189].

[9] A. De Rujula, S. L. Glashow, and U. Sarid, Nucl. Phys. **B** 333, 173 (1990).

[10] E. Zavattini *et al.* (PVLAS Collaboration) Phys. Rev. Lett. **96**, 110406 (2006) [arXiv: hep-ex/0507107].

[11] H. Gies, J. Jaeckel, and A. Ringwald, Phys. Rev. Lett. **97**, 140402 (2006) [arXiv: hep-ph/0607118].

[12] S.-J. Chen, H.-H. Mei, and W.-T. Ni (Q & A Collaboration), arXiv:hep-ex/0611050, submitted to Mod. Phys. Lett.; arXiv:hep-ex/0308071.

[13] G. Bertone, D. Hooper, and J. Silk, Phys. Rept. **405**, 279 (2005) [arXiv:hep-ph/0404175].

[14] D. N. Spergel *et al.*, [arXiv:astro-ph/0603449].

[15] J. A. Hinton [HESS Collaboration], New Astron. Rev. **48**, 331 (2004) [arXiv:astro-ph/0403052]; T. C. Weekes *et al.*, arXiv:astro-ph/9706143.

[16] P. Fayet, Phys. Rev. D **74**, 054034 (2006) [arXiv:hep-ph/0607318].

[17] O. Tajima *et al.* [Belle Collaboration], arXiv:hep-ex/0611041.

[18] J. Abdallah *et al.* [DELPHI Collaboration], Eur. Phys. J. C **38**, 395 (2005) [arXiv:hep-ex/0406019].

[19] Information is available at `http://www-cdf.fnal.gov/~harper/diEleAna.html`.